Chapter 1

SuperNEMO Demonstrator Sensitivity to Radon Background Measurement

The neutrinoless double beta decay decay is a very rare process. As such, for experiments that involve the search for $0\nu2\beta$ decay, it is particularly essential to mitigate the background. It is possible for any process that is capable of producing two electrons of high total energy close to $Q_{\beta\beta}$ (2.998 MeV for ^{82}Se) to mimic $0\nu2\beta$ decay, and thus contribute to the background. These processes originate mainly from isotopes capable of emitting high energy electrons or photons, in the natural ^{238}U and ^{232}Th decay chains.

Specific topologies and variables are chosen to suit the measurement of the main background. These variables are used to fit background contributions in a large number of pseudo-experiments in order to estimate the statistical and systematic uncertainties of different exposure times. In this chapter, the analysis strategy of characterising the background model of the SuperNEMO experiment is explained.

1.1 Radon As SuperNEMO Background

The signature of the $0\nu2\beta$ event is two electrons with energies that add up to the total decay energy $Q_{\beta\beta}$. There is an irreducible background from the high-energy tail of the $2\nu2\beta$. In addition, there are background events caused β-decaying isotopes: if the total energy released in a β decay is higher than the $Q_{\beta\beta}$ (2.99 MeV for the ^{82}Se used in this experiment), a second electron can be produced near the decay vertex via Møller or Compton scattering, or internal conversion, mimicking a $0\nu2\beta$ decay. The β decay background mainly comes from two sources: ^{214}Bi, ^{208}Tl within the source foil, and radon in the tracker gas. ^{214}Bi and ^{208}Tl are both β decaying isotopes with Q_β values of 3.27 MeV and 4.99 MeV, from the natural ^{238}U and ^{232}Th decay chains, respectively, see Figure 1.1. Due to their high Q_β, their decay can mimic the $0\nu2\beta$ signal, and experimentally this can be observed as a wide bump centred at 2.99 MeV ($Q_{\beta\beta}$ of ^{82}Se) when considering the the energy resolution of the calorimeter, and the energy loss of the electron as it leaves the foil and travels through the detector. Radon (^{222}Rn) is a supply of ^{214}Bi due to its long half-life and diffusion properties as a noble gas. While several approaches have been applied to ensure the radiopurity of the detector, a tiny amount of radon may still be present within the detector. For this reason, it essential to implement analysis tools for the identification and subsequent rejection of the background events.

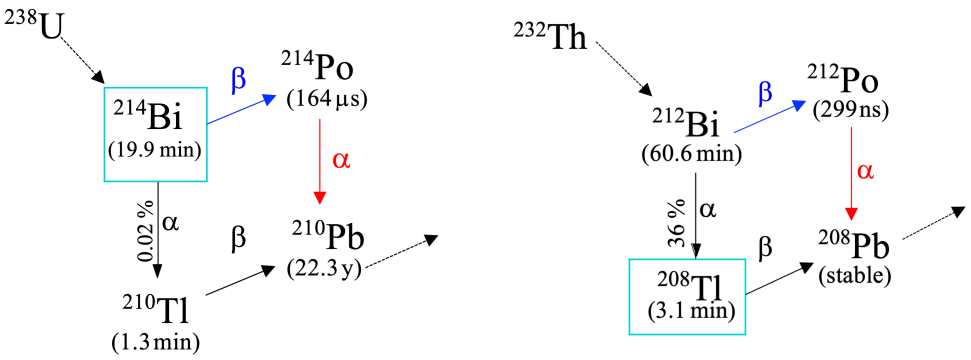

Figure 1.1: Beta decay of ^{214}Bi and ^{208}Tl are the major background of $0\nu2\beta$ searching experiments.

1.2 Radon Background Sensitivity Estimation via $1e1\alpha$

The background model of the experiment is built on the measurements of contributions from each part of the detector. The analysis is based on studying a large number of events with selected pure topology, which can provide an accurate determination of the contributions. The event of interest is the decay of ^{214}Bi nuclei on the field wire surface within the tracker volume. The ^{214}Bi contamination was measured by the delayed coincidence signature ~~was used to measure~~ the ^{214}Bi contamination, where ^{214}Bi β-decays to ^{214}Po, and then ^{214}Po quickly to α-decays to ^{210}Pb.

1.2.1 $1e1\alpha$ Topology

One significant advantage of the SuperNEMO tracker-calorimeter design is its ability to provide full reconstruction of individual partice tracks in order to identify the event topologies, which offers useful information on measuring the background. The most interesting topology for the SuperNEMO experiment are: 2e, 1e, 1eNγ, 2eNγ, 1eNα and, to a lesser extent 1e1p (one electron and one positron) [1]. Among them, the 1eNα topology is one of the most important analysis channels to measure the background of the SuperNEMO experiment.

To estimate the ^{214}Bi background in the tracker, a clean channel needs to be found to measure the ^{214}Bi. The BiPo decay chain, where ^{214}Bi β-decays to ^{214}Po, and then quickly to α-decays to ^{210}Pb (half-life 164.3μs), can be a clear signal in the identification of ^{214}Bi background events. These events can also be associated with no gammas, corresponding to a standard BiPo event where ^{214}Bi decays to the ground state of ^{214}Po, or n gammas (n¿0), corresponding to ^{214}Bi decaying to an excited state of ^{214}Po with one or a cascade of gammas emitted.

Since only ^{214}Bi events contribute to the $1e1\alpha$ topology, it would be one golden channel to measure the ^{214}Bi decay. The $1e1\alpha$ topology requires one electron track

with an associated calorimeter, and one alpha track with at least one Geiger hit. In addition, the vertex separation of the two particles should be less than 30 cm. **??**

All events can be classified into two selections based on the position of the reconstructed event vertex: the tracker selection in which the vertex locates in the tracker volume, and the source selection in which the event vertex is extrapolated to the source foil. As Falaise extrapolates the track to the foil during reconstruction, it is impossible to distinguish events with a vertex in the first layer of tracker and events from the foil,(see Figure 1.2). The reconstructed vertex is at the end of the electron track by definition.

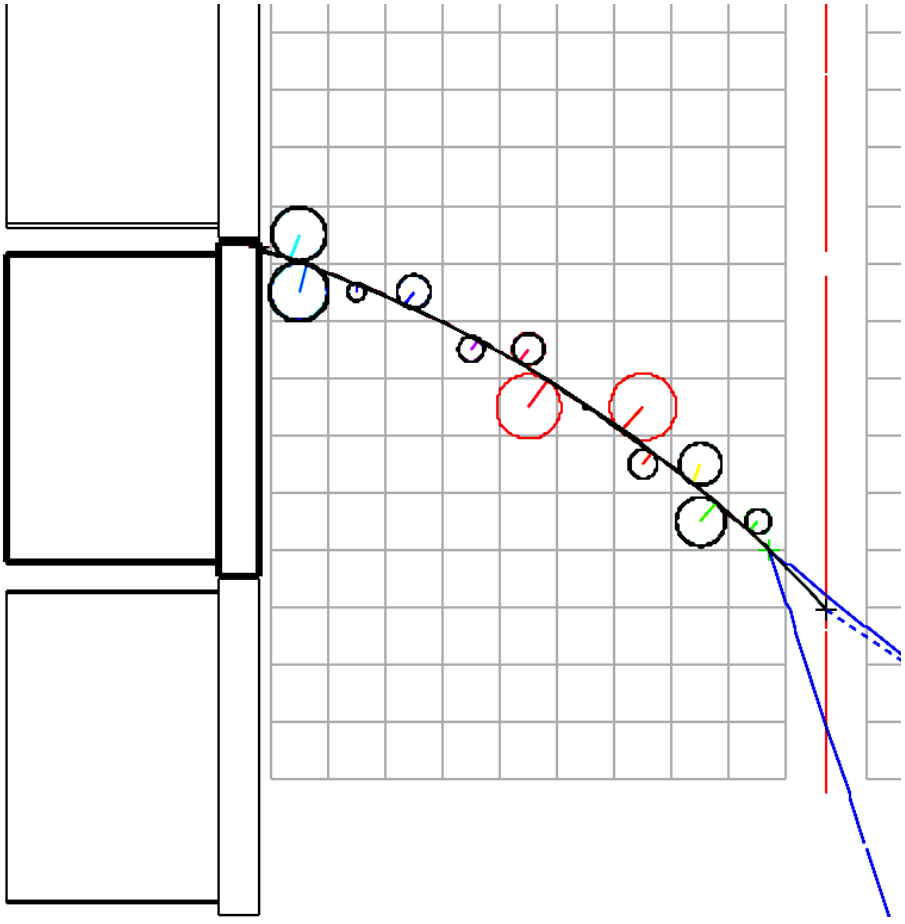

Figure 1.2: An event on the first layer of tracker was extrapolated to the foil during reconstruction, where the green cross is the true vertex and the black cross is the reconstructed vertex.

1.2.2 Event Number Estimation

The expected number of events N_i^{cut} depends on the activity A_i, detector acceptance and selection efficiency efficiency e_i^{cut}, and the exposure time T:

$$N_i^{cut} = e_i^{cut} \times A_i \times T \tag{1.1}$$

where i is the selection and can be either tracker or source selection, and the cut is normally made on topology which here is $1e1\alpha$.

1.2.3 Activity

The background of the source foil comes mainly from contamination of ^{214}Bi from the natural ^{238}U decay chain. The BiPo Detector [2] gives an upper limit of 4.94 mBq for the activity of Mylar, ^{82}Se source, and PVA in the source foils, and this value is used as the source foil bulk activity in the analysis. The BiPo detector was developed by the collaboration particularly to measure the impurities (^{214}Bi and ^{208}Tl contamination) in the source foils, where the foil is sandwiched by two thin layers of polystyrene scintillators and PMTs. C-Section Measurements using the RnCL have produced a tracker activity result of $41.3 \pm 4.7 mBq$ without flushing. For the SuperNEMO Demonstrator, by flushing at 1 m^3/h, a radon suppression factor of 9.71 can be achieved, as shown in Section **??**. These result in the tracker activity (with flushing) decreasing to 4.25 $\pm$ 0.48 mBq, or 0.28 $\pm$ 0.07 mBq/m^3. Since the decay daughters of radon are positively charged, due to the electric field, positive ^{214}Bi ions in the tracker gas to be attracted to the tracker field wires than the anode wires. In addition, it is assumed that positive ^{214}Bi ions in the gap (between the foil and the tracker first layer) are deposited on the surface of the source foil.

~~The decay daughters of radon are positively charged. Also, check the logic of the sentence: Bi214 is more likely to be positive and therefore attracted to field wires.~~

The total activity in the tracker gas is then split into two parts based on the gap and tracker volume ratio: 7.8% of the positive ^{214}Bi ions as deposited on the source

surface and the other 92.2% on wires, corresponding to an activity of 3.92 ± 0.44 mBq from the tracker wires and 0.34 ± 0.04 mBq from the surface of the source foil. Since the Mylar used as the source foil cover in SuperNEMO is different from that used in NEMO3, it is unclear how much radon will stick to it in real-life operation. As such, it is necessary to test various methods of splitting radon activity between the source foil surface mylar and the tracker field wires. These activities are summarised in Table 1.1.

detector components	activity	measured by detector
^{214}Bi in source foil bulk	4.94 mBq(upper limit)	BiPo detector
^{214}Bi in source foil surface	0.34 ± 0.44 mBq	RnCL
^{208}Tl in field wire surface	3.92 ± 0.44 mBq	RnCL

Table 1.1: ^{214}Bi and ^{208}Tl activities in the detector region. Results are from external measurements measured by the RnCL or the BiPo detector [2].

1.2.4 Samples

The three samples used in this study are ^{214}Bi events of which vertices are simulated randomly in source foil bulk, on source foil surface, and the tracker field wire surface. Each sample contains 1E6 events. It should be noted that the ^{214}Bi events from source foil bulk are from the contamination in the foil, and the ^{214}Bi events of from source foil surface, and the tracker field wire surface are from radon deposited on the surface areas. Two scenarios for the magnetic field are considered in the work of this thesis: 25 Gauss, and no field. Several cuts are applied to remove events from the data set if any of the following criteria are not satisfied:

- $1e1\alpha$ reconstructed topology requiring the event has only one electron, one alpha, and n gammas (n$\geq$0). In addition, at least one Geiger hit of the alpha particle must be a within 30 cm distance from the reconstructed vertex of the electron.

- An electron/positron candidate requires a reconstructed track with the associated calorimeter hit.

- Negative electron charge required for the 25 Gauss magnetic field scenario. No charge requirement for the no magnetic field scenario.
- An alpha candidate is defined by the delayed (¿10 μs) cluster of $\geq$ 1 tracker hit without associated calorimeter hit.
- Tracker selection, meaning the reconstructed event vertex should not be extrapolated to the source.

For the 25 Gauss magnetic field scenario, the magnetic field can bend electrons thus they can leave curved tracks, but not strong enough to bend alphas. Also, for high energy electrons ($>$ 2 MeV) the bend is often indistingushible. The negative or positive charge of the electron or position can be determined by the helices of the track (positive charge curved, negative charge curved, or straight). For the no magnetic field scenario, it is impossible to tell the charge of an electron/positron candidate which has a reconstructed track with the associated calorimeter hit. Thus all the candidates which have one reconstructed track and an associated calorimeter hit, are accepted as electrons. The SuperNEMO calorimeter has an instrumental energy threshold of 50 keV, ~~thus all the calorimeter hit has an energy above 50 keV.~~ The cut flow efficiencies are summarised in Table 1.2 to 1.7. In table, 1 e and 1 α means the event has only 1 electron candidate, 1 alpha candidate and no extra track of other particle. And the 1e1α topology has further requirement on the vertex seperation of the electron and alpha particle to be a less than 30 cm.

1.2.5 Alpha Track Length Distribution

The SuperNEMO demonstrator detector can measure the background contributions independently from previous external measurements, such as the RnCL, Germanium detector, and BiPo detector measurements Section **??**. Finding a suitable discriminating variable will be essential in enabling the measurement of background levels within the detector. The reconstructed alpha track length is chosen as the discriminating observable to distinguish the background events from different detector

events true vertex region	number of events	efficiency
$\geq$ 1 calorimeter hit	849663	84.97%
$\geq$ 1 reconstructed track	702078	70.21%
1 electron/positron candidate	451161	45.12 %
1 e (negative charged)	404640	40.46 %
1 e and $\geq$ 1 delayed tracker hit	37843	3.78 %
1 e and 1 α (no other track)	27108	2.71%
1e1α topology	20731	2.07%
1e1α & electron vertex in tracker	656	0.07%

Table 1.2: 1e1α channel cut flow of the selection efficiency for 25 Gauss magnetic field Tracker ^{214}Bi from source bulk

events true vertex region	number of events	efficiency
$\geq$ 1 calorimeter hit	846445	84.64%
$\geq$ 1 reconstructed track	783841	78.38%
1 electron/positron candidate	452729	45.27 %
1 e (negative charged)	404187	40.42 %
1 e and $\geq$ 1 delayed tracker hit	129185	12.92%
1 e and 1 α (no other track)	98591	9.86%
1e1α topology	92569	9.26%
1e1α & electron vertex in tracker	2251	0.23%

Table 1.3: 1e1α channel cut flow of the selection efficiency for 25 Gauss magnetic field Tracker ^{214}Bi from source surface. 1E6 enevts generated for each component.

events true vertex region	number of events	efficiency
$\geq$ 1 calorimeter hit	849876	84.99%
$\geq$ 1 reconstructed track	787558	78.76%
1 electron/positron candidate	398650	39.87 %
1 e (negative charged)	299084	29.91 %
1 e and $\geq$ 1 delayed tracker hit	157978	15.80 %
1 e and 1 α (no other track)	80278	8.03%
1e1α topology	72447	7.24%
1e1α & electron vertex in tracker	54342	5.43%

Table 1.4: 1e1α channel cut flow of the selection efficiency for 25 Gauss magnetic field Tracker ^{214}Bi from field wire surface. 1E6 enevts generated for each component.

events true vertex region	number of events	efficiency
$\geq$ 1 calorimeter hit	861045	86.10%
$\geq$ 1 reconstructed track	712993	71.30%
1 electron candidate	497653	49.77 %
1 e and $\geq$ 1 delayed tracker hit	46094	4.60 %
1 e and 1 α (no other track)	34415	3.44%
1e1α topology	26054	2.61%
1e1α & electron vertex in tracker	534	0.05%

Table 1.5: 1e1α channel cut flow of the selection efficiency for no magnetic field Tracker ^{214}Bi from source bulk

events true vertex region	number of events	efficiency
$\geq$ 1 calorimeter hit	857906	85.79%
$\geq$ 1 reconstructed track	788478	78.85%
1 electron candidate	486201	48.62%
1 e and $\geq$ 1 delayed tracker hit	155159	15.52%
1 e and 1 α (no other track)	122533	12.25%
1e1α topology	115248	11.52%
1e1α & electron vertex in tracker	1927	0.19%

Table 1.6: 1e1α channel cut flow of the selection efficiency for no magnetic field Tracker ^{214}Bi from source surface. 1E6 enevts generated for each component.

events true vertex region	number of events	efficiency
$\geq$ 1 calorimeter hit	851205	85.12%
$\geq$ 1 reconstructed track	786418	78.64%
1 electron candidate	401313	40.13%
1 e and $\geq$ 1 delayed tracker hit	209349	20.93%
1 e and 1 α (no other track)	112666	11.27%
1e1α topology	98435	9.84%
1e1α & electron vertex in tracker	75891	7.59%

Table 1.7: 1e1α channel cut flow of the selection efficiency for no magnetic field Tracker ^{214}Bi from field wire surface. 1E6 enevts generated for each component.

region. Alpha particles emitted from the tracker wire surface do not need to travel through the dense source, in contrast to alphas within the source. For this reason, alphas emitted in the source bulk will lose some energy as they pass through the source material prior to detection by the tracker, resulting in shorter tracks than those by alphas emitted within the traker. The alpha track length distribution of three different components are studied, as shown in Figure 1.3..

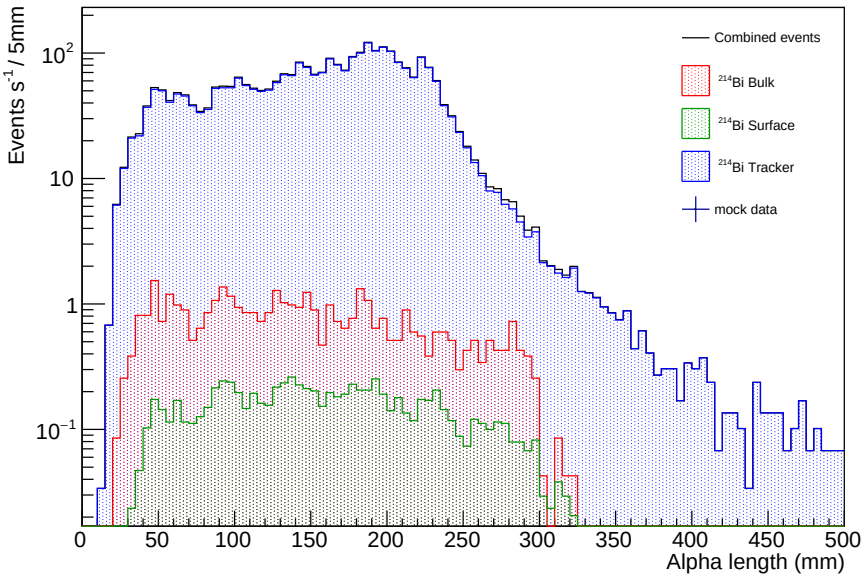

Figure 1.3: A Monte-Carlo simulation of α *track length distributions from three locations of the* ^{214}Bi background corresponding to 60 day of data taking.

The three distributions of alpha track lengths are normalised to their respective activities provided by external measurements. The alpha track length distribution can be further normalised to the specific exposure of a pseudo experiment to obtain a final distribution.

1.2.6 Pseudo-experiments

To identify how much data required to carry out a radon measurement in the tracker with a particular accuracy, 5% here, pseudo-experiments are generated from the final alpha track length distribution in order to provide datasets similar to what will be measured during real operation of the demonstrator detector. To mimic the

real data, the number of expected events is a random number in accordance with the Poisson distribution. The pseudo-experiment datasets are fitted with the three distributions from the three components, using a binned normalisation fit to return the activity of each component. Here, we focus on events on the tracker field wire surface. An example of pseudo-experiment with the best fit is shown in Figure 1.4.

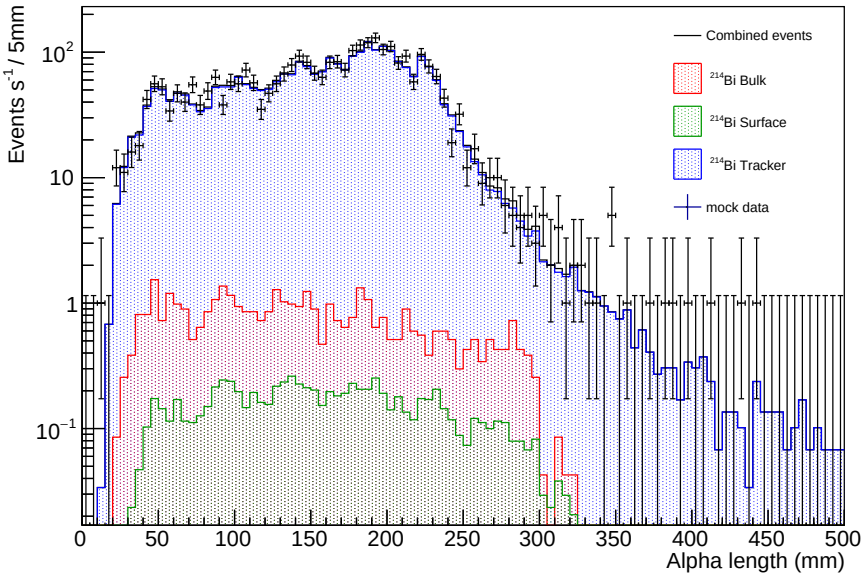

Figure 1.4: Data from a pseudo-experiment fitted with α track length distributions for $1e1\alpha$ events.

1.2.7 Activity Measurement

The pseudo experiment is repeated a large number times (1E5 time here), in order to evaluate the stability of the approach and determine the statistical uncertainty. The distribution of the activities measured for each pseudo-experiment, running for specific exposure times, are presented in Figure 1.5 for the ^{214}Bi component on the tracker field wire surface. The distributions of the measured ^{214}Bi activities on the field wire surface for each pseudo experiment are fitted with Gaussian functions, with one standard deviation taken as the uncertainty on the measurement. The mean ^{214}Bi activities are well within 1% of their expected values which are provided using inputs from independent measurements with external detectors such as the RnCL, the HPGe[3] and the BiPo detector.

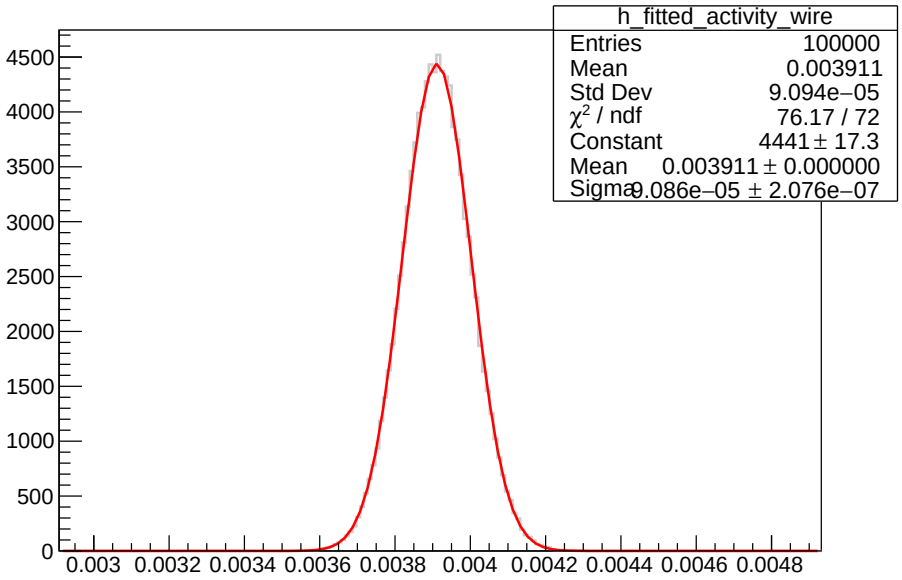

Figure 1.5: Distribution of the ^{214}Bi activities in the tracker measured from the pseudo-experiments (days, exposure kgyr).$True value of the ^{214}$Bi activities is 3.92 mBq.

1.2.8 Sensitivity Dependence on the Exposure Time

To investigate the evolution of the relative errors with time, the pseudo-experiments can be generated for various exposure times. For the tracker selection, the relative error as a function of exposure time is shown in Figure 1.6, and Figure 1.7 for 25 Gauss magnetic field, and no magnetic field respectively.

Using the efficiency from the reconstruction of the $1e1\alpha$ channel and the externally measured activities of the detector components, the expected background level due to ^{222}Rn can be computed. The level of ^{222}Rn coming from the tracker can be determined at 5% after 12 days of measurement; it can thus be measured reasonably quickly via the $1e1\alpha$ channel.

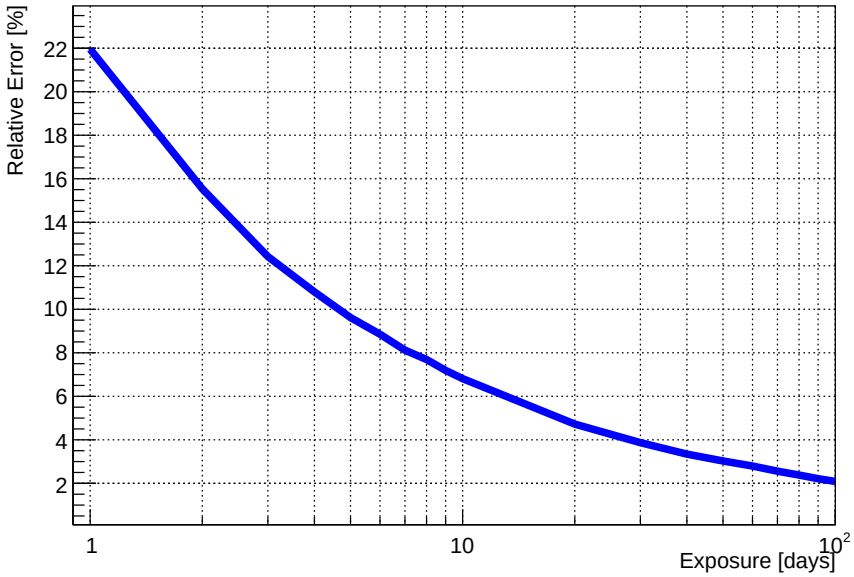

Figure 1.6: Relative error on the Rn content measurement in the SuperNEMO tracker as a function of the exposure (measurement time) using $1e1\alpha$ channel for the case of a 25 Gauss magnetic field.

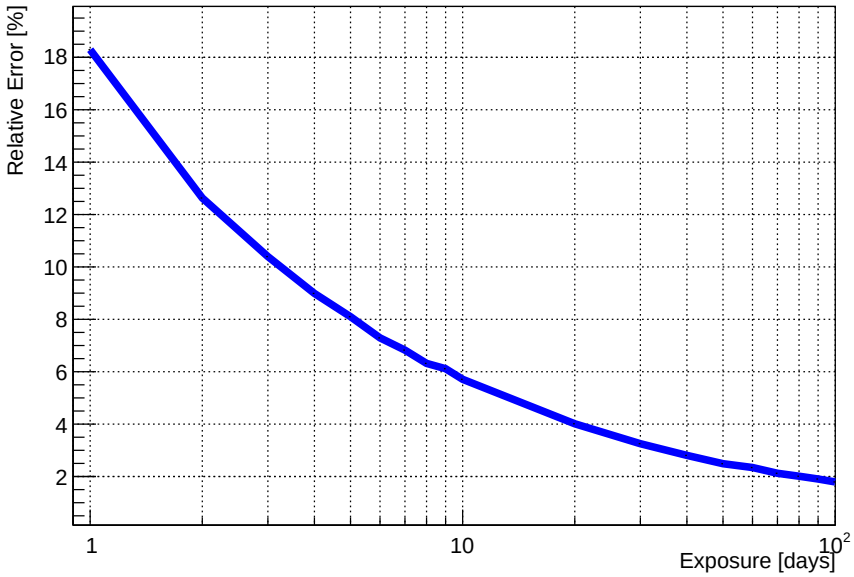

Figure 1.7: Relative error on the Rn content measurement in the SuperNEMO tracker as a function of the exposure (measurement time) using $1e1\alpha$ channel for the case of no magnetic field..

Bibliography

[1] S. Calvez. *Development of reconstruction tools and sensitivity of the SuperNEMO demonstrator*. PhD thesis, l'Université Paris-Saclay préparée à l'Université Paris-Sud, 2017.

[2] S. Cebrian. The BiPo detector. *Internal Note*, DocDB:894, 2009.

[3] X. R. Liu. *Low background techniques for the SuperNEMO experiment*. PhD thesis, University College London, 2017.